Array-Aided CORS Network Ambiguity Resolution

Bofeng Li and Peter J.G. Teunissen

Abstract

Array-aided precise point positioning (A-PPP) is a measurement concept that uses Global Navigation Satellite System (GNSS) data, from multiple antennas in an array of known geometry, to realize the improved GNSS parameter estimation. In this contribution the ambiguity resolution benefits of A-PPP for antenna-array equipped CORS stations is explored. To demonstrate the performance of array-aided ambiguity resolution between-station, an 80 km baseline experiment, equipped with a 6-antenna array at each CORS station, was conducted. We formulate the underlying model, show how the array-data to be reduced and present numerical results on the ambiguity resolution performance. The results show that the use of antenna-arrays can significantly improve the CORS network ambiguity resolution.

Keywords

A-PPP • Antenna-array • Ambiguity resolution • Success-rate • Bootstrapping

1 Introduction

Integer ambiguity resolution (IAR) is the key to high precision GNSS (Global Navigation Satellite System) applications. It improves the precision of the estimated model parameters by about two orders of magnitude. For positioning, successful IAR effectively transforms the estimated fractional carrier-phases into ultra-precise receiver-satellite ranges, thus making high-precision positioning possible. However, the success of IAR depends on the strength of the underlying GNSS model. The weaker the model, the more observation epochs need to be accumulated before IAR can be successful and the more time it therefore takes before one can profit from the ultra-precise carrier signals. Clearly, the aim is to shorten the time-to-fix, preferably to zero, thereby enabling truly instantaneous GNSS positioning.

Traditionally, single-baseline IAR is based on data of two stations, each equipped with one antenna only. However, if each station would be equipped with an array of antennas with known geometry in the body-frame, then the GNSS observations from these multiple antennas can be used to significantly improve parameter estimation. This measurement concept, due to Teunissen (2012), is referred to as array-aided precise point positioning (A-PPP). This concept has also been applied to attitude determination and formation flying (Buist et al. 2011).

In Teunissen (2012), it was suggested to use antenna-arrays for improving CORS (Continuously Operating Reference Station) capabilities such as CORS network ambiguity resolution. In this contribution, a case study will be carried out to explore the benefits of such array-aided CORS network

B. Li (✉)
College of Surveying and Geo-Informatics, Tongji University, Shanghai, P.R. China

GNSS Research Center, Department of Spatial Sciences, Curtin University, Bentley, Australia
e-mail: bofeng_li@tongji.edu.cn; bofeng.li@curtin.edu.au

P.J.G. Teunissen
GNSS Research Centre, Department of Spatial Sciences, Curtin University, Bentley, Australia

Delft Institute of Earth Observation and Space Systems (DEOS), Delft University of Technology, Delft, The Netherlands
e-mail: p.teunissen@curtin.edu.au

C. Rizos and P. Willis (eds.), *Earth on the Edge: Science for a Sustainable Planet*, International Association of Geodesy Symposia 139, DOI 10.1007/978-3-642-37222-3_79,

Fig. 1 The layout of antenna-array at two platforms, r_0 and b_0, of one baseline. An array of antennas, $r_1,\ r_2,\ \cdots,\ r_n$, are mounted on the platform r_0, and the antennas, $b_1,\ b_2,\ \cdots,\ b_n$ on the platform b_0

ambiguity resolution. An 80 km baseline experiment was conducted for which both stations were equipped with a 6-antenna array. We formulate the corresponding array-aided CORS (AAC) model and apply the principle of multivariate mixed integer least-squares estimation. Using the success-rate of ambiguity resolution as performance measure, the improved strength of the AAC model will be examined under varying scenarios, i.e., using different standard deviations for the ionospheric constraints, different number of observation epochs, as well as different number of antennas in the array.

The rest of this contribution is organized as follows. In Sect. 2, the AAC principle is described in brief. In Sect. 3, the multivariate AAC model is presented. Then the steps of generating reduced observations are given in Sect. 4. The experiment and results are presented in Sect. 5 and finally, the conclusions are given in Sect. 6.

2 Principle of Array-Aided Ambiguity Resolution

The principle of array-aided ambiguity resolution is briefly sketched in this section. As shown in Fig. 1, two stations (with platform), r_0 and b_0, form a baseline for which the double-differenced (DD) ambiguities need to be resolved. Traditionally, only one antenna is used at each of two baseline stations, while in A-PPP mode, each station is equipped with a platform of more than one antenna. The antennas, $r_1,\ r_2,\ \cdots,\ r_n$ are mounted on platform r_0, and the antennas, $b_1,\ b_2,\ \cdots,\ b_n$, on platform b_0. Importantly, the geometry of the antenna configuration on each platform is assumed known in the platform body-frame. This known antenna-array geometry allows one then to reduce the observations from the array antennas to a set of observations that can be thought to belong to a single virtual antenna. The reduction of the platform phase measurements requires ambiguity resolution over the baselines formed by array antennas on the platform. This, fortunately, is possible with high success-rate due to the known geometry of the antenna-array.

Since the reduced observations can be seen as being the result of an adjustment, their precision is better than that of the original observations from the individual antenna. Therefore, improved ambiguity resolution can be expected when the $r_0 - b_0$ baseline ambiguity resolution is based on these reduced observations.

3 The Multivariate Array-Aided CORS Model

In this section, we present the multivariate array-aided CORS model and show how it can be solved. In the following, I_n denotes the unit matrix of order n, c_1 is a unit vector with its 1 in the first slot and e_n is an n-vector of 1s; $\otimes$ denotes the Kronecker product while $\mathtt{vec}$ the vectorizing operator. $\mathtt{E}$ and $\mathtt{D}$ denote the mathematic operations of expectation and dispersion, respectively.

3.1 Functional Model of Multivariate SD Observations

The single-frequency, single-epoch, between-satellite single-differenced (SD) observation equations of phase and code read

$$\begin{aligned} \mathtt{E}(\phi_{r,j}) &= G_r x_r - \mu_j \iota_r + \tau_r - \delta t_{,j} + \lambda_j a_{r,j} \\ \mathtt{E}(p_{r,j}) &= G_r x_r + \mu_j \iota_r + \tau_r - dt_{,j} \end{aligned} \tag{1}$$

where the subscripts r and j denote the antenna and the frequency f_j (with wavelength λ_j), respectively. With the assumption that $(s+1)$ satellites are simultaneously tracked, G_r is the $(s \times 3)$ coefficient matrix of the (3×1) baseline unknown x_r; $\phi_{r,j} = [\phi^1_{r,j}, \cdots, \phi^s_{r,j}]^T$ and $p_{r,j} = [p^1_{r,j}, \cdots, p^s_{r,j}]^T$ are the SD phase and code observation vectors; $\iota_r = [\iota^1_r, \cdots, \iota^s_r]^T$ is the vector of SD ionospheric delays on frequency f_1, with $\mu_j = f_1^2/f_j^2$; $\delta t_{,j} = [\delta t^1_{,j}, \cdots, \delta t^s_{,j}]^T$ and $dt_{,j} = [dt^1_{,j}, \cdots, dt^s_{,j}]^T$ are the SD satellite clock errors of phase and code, respectively; $a_{r,j} = [a^1_{r,j}, \cdots, a^s_{r,j}]^T$ is the SD ambiguity vector with the sth element $a^s_{r,j} = z^s_{r,j} - \varphi^s_{,j}(t_0)$, where $z^s_{r,j}$ is integer and $\varphi^s_{,j}(t_0)$ is real-valued; $\tau_r = [\tau^1, \cdots, \tau^s_r]^T$ is the vector of SD tropospheric delays. The superscripts in all terms above denote the number of SD observation.

If we combine the SD observation equations on all f frequencies, we may write

$$\mathrm{E}(y_r) = M_r x_r + N a_r + \nu \otimes \iota_r + e_{2f} \otimes \tau_r - \theta_r \quad (2)$$

where $y_r = [\phi_r^T,\ p_r^T]^T$, $\phi_r = [\phi_{r,1}^T, \cdots, \phi_{r,f}^T]^T$; $M_r = e_{2f} \otimes G_r$, $\nu = [-1,\ 1]^T \otimes \mu$ with $\mu = [\mu_1, \cdots, \mu_f]^T$, $N = [1,\ 0]^T \otimes \Lambda \otimes I_s$ with $\Lambda = \mathrm{diag}(\lambda_1, \cdots, \lambda_f)$; $\theta_r = [\delta t^T,\ dt^T]^T$, $\delta t = [\delta t_{,1}^T, \cdots, \delta t_{,f}^T]^T$; p_r and a_r have the same structures as ϕ_r, while dt the same structure as δt.

Since the distance between the antennas on the platform is short (in our case shorter than 1 m), the atmospheric delays of all antennas on the platform to one satellite are equal and the same relative receiver-satellite geometry coefficient matrix can be used for each antenna on the platform. Hence, $M = M_i$, $\tau = \tau_i$ and $\iota = \iota_i$ $(i = 1, \cdots, r)$, and the multivariate set of SD observation equations for the r platform antennas reads

$$\mathrm{E}(Y) = MX + \nu \otimes (e_r^T \otimes \iota) + NA + e_{2f} \otimes (e_r^T \otimes \tau) - \Theta \quad (3)$$

where $Y = [y_1, \cdots, y_r]$, $X = [x_1, \cdots, x_r]$, $A = [a_1, \cdots, a_r]$ and $\Theta = [\theta_1, \cdots, \theta_r]$. Defining a square matrix of full-rank $R_r = [c_1,\ D_r]$ with $D_r^T = [-e_{r-1},\ I_{r-1}]$, we can transform (3) without any information loss by post-multiplying it with R_r

$$\mathrm{E}(YR_r) = \mathrm{E}\begin{bmatrix} y_1 & \tilde{Y} \end{bmatrix} = \begin{bmatrix} Mx_1 + Na_1 + \beta_1 & M\tilde{X} + N\tilde{Z} \end{bmatrix} \quad (4)$$

where $\beta_1 = \nu \otimes \iota + e_{2f} \otimes \tau - \theta_1$, $\tilde{Y} = YD_r = [y_{12}, \cdots, y_{1r}]$, $\tilde{X} = XD_r = [x_{12}, \cdots, x_{1r}]$, $Z = AD_r = [z_{12}, \cdots, z_{1r}]$. Here $(\bullet)_{ij} = (\bullet)_j - (\bullet)_i$. Note that now all entries in Z are integer.

3.2 Stochastic Model of Multivariate SD Observations

We start from the stochastic model of single-frequency, single-epoch undifferenced observations

$$\mathrm{D}\begin{bmatrix} \tilde{\phi}_{r,j} \\ \tilde{p}_{r,j} \end{bmatrix} = \begin{bmatrix} \sigma_{\phi;j}^2 & 0 \\ 0 & \sigma_{p;j}^2 \end{bmatrix} \otimes Q_{0,r} \quad (5)$$

where $\tilde{\phi}_{r,j}$ and $\tilde{p}_{r,j}$ are the undifferenced phase and code observations. $Q_{0,r}$ is the elevation-dependent cofactor matrix of single-frequency, single-epoch undifferenced observations; $\sigma_{\phi;j}^2$ and $\sigma_{p;j}^2$ are the variance scalars of phase and code on frequency j, respectively. The cross-correlation between phase and code is assumed non-existent. Then the stochastic model of (1) is

$$\mathrm{D}\begin{bmatrix} \phi_{r,j} \\ p_{r,j} \end{bmatrix} = \begin{bmatrix} \sigma_{\phi;j}^2 & 0 \\ 0 & \sigma_{p;j}^2 \end{bmatrix} \otimes D_s^T Q_{0,r} D_s \quad (6)$$

with the between-satellite differencing matrix $D_s^T = [-e_s,\ I_s]$ (satellite 1 is chosen here as reference satellite). The stochastic model of (2) is

$$\mathrm{D}(y_r) = Q_{y_r} = S \otimes D_s^T Q_{0,r} D_s \quad (7)$$

where $S = \mathrm{blockdiag}(S_\phi,\ S_p)$, $S_\phi = \mathrm{diag}(\sigma_{\phi;1}^2, \cdots, \sigma_{\phi;f}^2)$ and $S_p = \mathrm{diag}(\sigma_{p;1}^2, \cdots, \sigma_{p;f}^2)$. Then the stochastic model of the multivariate SD model (3) reads

$$\mathrm{D}(\mathrm{vec}(Y)) = \mathrm{blockdiag}(Q_{y_1}, \cdots, Q_{y_r}) \quad (8)$$

If the same type of antennas are used on the platform, then $Q_0 = Q_{0;i}$, $Q_y = Q_{y_i} = S \otimes D_s^T Q_0 D_s$ $(i = 1, \cdots, r)$ and (8) becomes

$$\mathrm{D}(\mathrm{vec}(Y)) = I_r \otimes Q_y \quad (9)$$

With this result, the variance-covariance matrix of (4) becomes

$$\mathrm{D}(\mathrm{vec}(YR_r)) = \begin{bmatrix} 1 & c_1^T D_r \\ D_r^T c_1 & D_r^T D_r \end{bmatrix} \otimes Q_y \quad (10)$$

where $c_1^T c_1 = 1$ has been used for the first element.

3.3 The Multivariate CORS Model in Decorrelated Form

From (10) it follows that y_1 and $\tilde{Y}$ of (4) are correlated. As shown by Teunissen (2012), the CORS model can be written in equivalent, but decorrelated, form as

$$\mathrm{E}\begin{bmatrix} \bar{y} \\ \tilde{Y} \end{bmatrix} = \begin{bmatrix} M\bar{x} + N(a_1 + \bar{z}) + \beta_1 \\ M\tilde{X} + N\tilde{Z} \end{bmatrix} \quad (11)$$

with $\bar{y} = \sum_{i=1}^r y_i/r$, $\bar{x} = \sum_{i=1}^r x_i/r$ and $\bar{z} = \sum_{i=2}^r z_{1i}/r$. The dispersion of $\bar{y}$ and $\tilde{Y}$ then follows

$$\mathrm{D}\left(\begin{bmatrix} \bar{y} \\ \mathrm{vec}(\tilde{Y}) \end{bmatrix}\right) = \begin{bmatrix} 1/r & 0 \\ 0 & D_r^T D_r \end{bmatrix} \otimes Q_y \quad (12)$$

Note that $\bar{y}$ is r-times more precise than y_1. Furthermore, as shown in Teunissen (2012), the given geometry of the antenna configuration allows for the integer matrix estimator $\check{Z}$ of Z to be determined with a very high success-rate from $\mathrm{E}(\tilde{Y}) = M\tilde{X} + N\tilde{Z}$. Hence, for all practical purposes one may assume Z known and therefore also $\bar{z} = \frac{1}{r} Z e_{r-1}$ of the first equation of (11) known.

Since $\bar{x}$ and $\bar{z}$ may be assumed known, the reduced observation equation of a CORS station can now be written in the two remaining unknowns a_1 and β_1 as $\mathrm{E}(\bar{y} - M\bar{x} - N\bar{z}) = Na_1 + \beta_1$. For two CORS stations, say P and Q, the between-CORS observation equation reads then

$$\mathrm{E}(\bar{y}_{\mathrm{PQ}}) = Nz_{\mathrm{PQ}} + \beta_{\mathrm{PQ}} \tag{13}$$

with the very precise reduced observable $\bar{y}_{\mathrm{PQ}} = \bar{y}_{\mathrm{Q}} - \bar{y}_{\mathrm{P}} - M(\bar{x}_{\mathrm{Q}} - \bar{x}_{\mathrm{P}}) - N(\bar{z}_{\mathrm{Q}} - \bar{z}_{\mathrm{P}})$, the integer ambiguity vector $z_{\mathrm{PQ}} = a_{1\mathrm{Q}} - a_{1\mathrm{P}}$ and $\beta_{\mathrm{PQ}} = \beta_{1\mathrm{Q}} - \beta_{1\mathrm{P}}$. This shows how between-CORS ambiguity resolution (i.e. the integer estimation of z_{PQ}) can benefit from the antenna-array and in particular from r, the number of antennas in the array.

4 The Steps for Reducing the CORS Antenna-Array Data

In this section we summarize the steps that need to be followed for reducing the CORS antenna-array data. We describe it for the single-frequency case, which is however easily generalized to the multi-frequency case.

1. Load the single-epoch phase $\tilde{\phi}_r^s$ and code $\tilde{p}_r^s$ observations of all antennas in the array.
2. Form the DD observations, using antenna 1 and satellite 1 as reference, and construct the data matrix $\tilde{Y}$.
3. Solve for the integer ambiguity matrix Z of the multivariate array-aided CORS model

$$\mathrm{E}(\tilde{Y}) = M\tilde{X} + NZ \tag{14}$$

   Since it is crucial that Z can be estimated with sufficiently high success-rate (also in the single-frequency case), special precautions need to be taken. The high success-rate can be achieved when making use of the antenna-geometry. If this geometry is known in the body-frame, then the MC-LAMBDA method can be applied to achieve high success-rate, see e.g. Teunissen (2010) and Giorgi et al. (2010). In case $\tilde{X}$ is completely known (e.g. in ECEF- or NEU-frame), then even the standard LAMBDA method (Teunissen 1995) can be applied to integer estimate Z with high success-rate. In that case one may even opt for the easier-to-applied integer bootstrapping or integer rounding methods, provided they are applied to the decorrelated ambiguities.
4. Using the entries of the integer estimated ambiguity matrix $\check{Z} = [\check{z}_{12}, \ldots, \check{z}_{1r}]$, the undifferenced phase and code measurements can be reduced as

$$\bar{\phi}^s = \sum_{i=1}^{r} (\tilde{\phi}_i^s - \lambda \check{z}_{1i}^{1s})/r \quad , \quad \bar{p}^s = \sum_{i=1}^{r} \tilde{p}_i^s / r \tag{15}$$

5 Experiment and Analysis

5.1 The CORS Antenna-Array Platform

The CORS platforms used for our experiment are of the type shown in Fig. 2. We collected dual-frequency GPS data on a 80 km baseline in the Perth area, West Australia, for a period of 17 h using a sampling interval of 5 s. Figure 3 shows the sky-plot of all tracked satellites during the observation time span.

Our platforms were equipped with Sokkia (receiver type: GSR2700 ISX, antenna type: Internal Pinwheel$^{\mathrm{TM}}$) and Javad (receiver type: Javad Delta, antenna type: GrAnt-G3T) receivers. We made sure that code-smoothing was turned off to cancel the time correlation of observations. In terms of Li et al. (2008), the standard deviations of all observation types for two types of receivers were determined as shown in Table 1. In the baseline processing, using the reduced CORS data with 15° elevation cut-off, the coordinates of the two CORS stations were assumed known. Hence, the remaining unknown DD parameters were the atmospheric delays and the ambiguities, referring to (13). The ionosphere-weighted model was used with a zenith tropospheric delay (ZTD). In the following the ambiguity fixing efficiency (fix-rate) and its reliability (two types of errors) of array-aided mode will be analyzed by comparing with those of conventional ambiguity resolution mode.

5.2 Fix-Rate of Array-Aided Ambiguity Resolution

To analyze the ambiguity resolution performance, various scenarios were examined by using the different number of antennas on the platform (1, 2, 4 and 6), the different number of data epochs (from 1 to 10) and the different standard deviations for the ionospheric constraints (the DD ionospheric standard deviation was set at 10, 15, 20 cm, and ∞). For these scenarios we evaluated the fix-rates based on the bootstrapped success-rate. The fix-rate is defined as the occurrence frequency of solutions having larger than 99.9 % bootstrapped success-rate:

$$P_{\mathrm{fix}} = \frac{\#\text{ solutions with } P_B > 99.9\%}{\text{total }\#\text{ solutions}} \tag{16}$$

with the bootstrapped success-rate computed as

$$P_B = \prod_{i=1}^{m} \left(2\Phi\left(\frac{1}{2\sigma_{\hat{z}_{i|I}}}\right) - 1 \right) \tag{17}$$

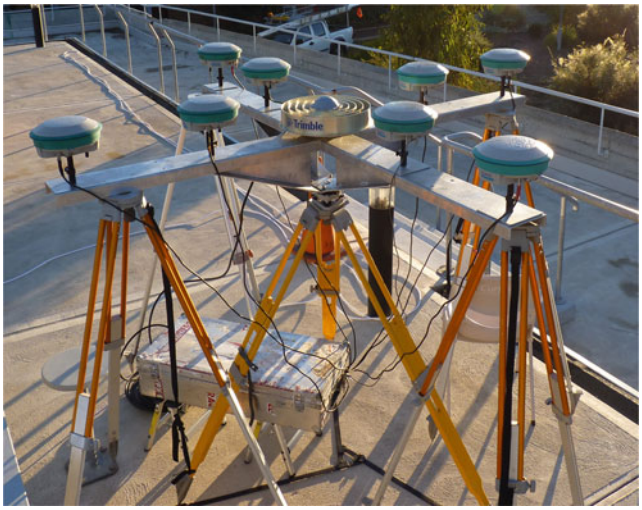

Fig. 2 The antenna-array platform used in our experiment

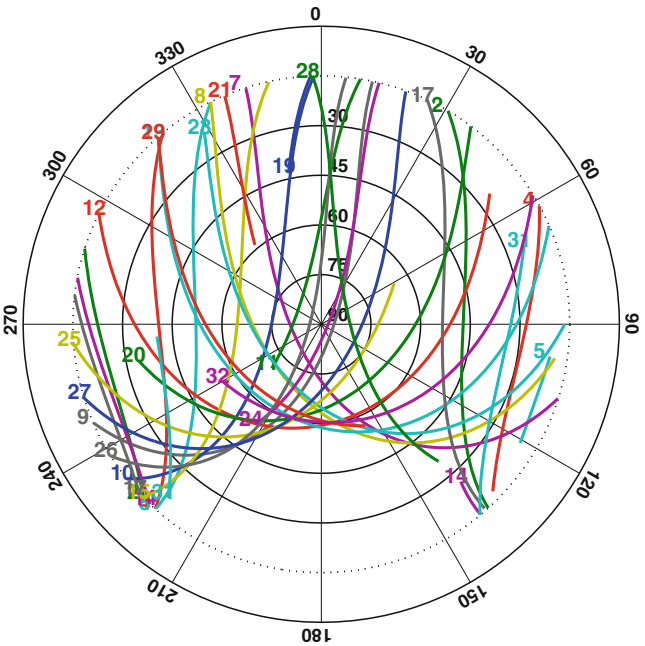

Fig. 3 The sky-plot of all tracked satellites during the observation time span

Table 1 Standard deviations of Sokkia and Javad data

Antenna	L1 (mm)	L2 (mm)	C1 (cm)	P2 (cm)
Sokkia	2.3	3.2	30	42
Javad	2.1	3.3	25	22

where

$$\Phi(x) = \int_{-\infty}^{x} \frac{1}{\sqrt{2\pi}} e^{-\frac{t^2}{2}} \, \mathrm{d}t$$

and $\sigma_{\hat{z}_{i|I}}$ is the conditional standard deviation of the ith decorrelated float ambiguity conditioned on the $(i-1)$ previous decorrelated float ambiguities ($I = \{1, \cdots, (i-1)\}$). The conditional variances are the entries of the diagonal matrix in the triangular decomposition of the decorrelated variance-covariance matrix $Q_{\hat{z}\hat{z}}$. We remark that this bootstrapped success-rate is a sharp lower bound of the integer least-squares success-rate (Teunissen 1998; Verhagen et al. 2013).

The fix-rates are shown in Fig. 4, for the different scenarios, as function of the number of data epochs used. The results show that:

- the fix-rate, as expected, improves when more antennas, more data epochs and smaller ionospheric standard deviation are used;
- single-epoch ambiguity resolution is impossible, not only for the ionosphere-float model, but also for the cases when the number of antennas is less than 4, even if the standard deviation of SD ionospheric constraint is as small as 10 cm. However, if more antennas are involved, single-epoch ionosphere-weighted ambiguity resolution becomes possible, albeit with a low fix-rate (at most 47 % with six antennas);
- with more antennas, a steeper fix-rate improvement can be achieved when the number of data epochs increases. This becomes more markedly the weaker the a-priori ionospheric constraint becomes;
- the fix-rate of more antenna is more immune to the strength of ionospheric constraint. In the absence of any ionospheric constraints (i.e. ionosphere-float case), a 6-antenna array can achieve a 99 % fix-rate in six epochs. For a single antenna, this fix-rate would still be practically zero.

5.3 Efficiency and Reliability of Array-Aided Ambiguity Resolution

P_{fix} of (16) describes the occurrence frequency of $P_B > 99.9\,\%$. As such it is a measure of strength of the multivariate array-aided CORS model during the experiment time span. As demonstrated in the previous section, the strength of the multivariate array-aided model significantly increases when multiple antennas in known configuration are used. One would expect that this also pays off in an improved efficiency and reliability of ambiguity resolution. This is indeed the case as the following shows.

In analogy with the concepts of type I errors (i.e., rejecting a correct solution) and type II errors (i.e., accepting an incorrect solution) (Koch 1999; Teunissen 2006), we define

$$P_{\text{I}} = \frac{\#\text{ rejected } (P_B < 99.9\%) \text{ but correct solutions}}{\#\text{ rejected solutions with } P_B < 99.9\%} \tag{18}$$

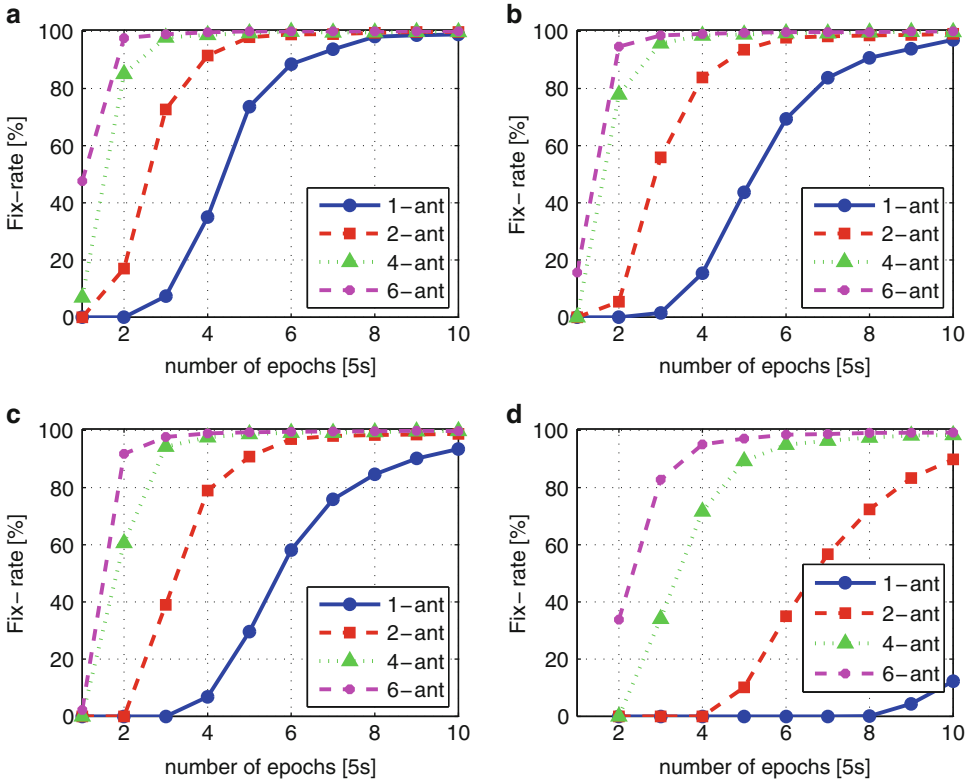

Fig. 4 The fix-rate P_{fix} (based on $P_B > 99.9\,\%$) as function of number of epochs. The subplots (**a**–**d**) represent the results obtained with the DD ionospheric standard deviations, 10, 15, 20 cm and ∞

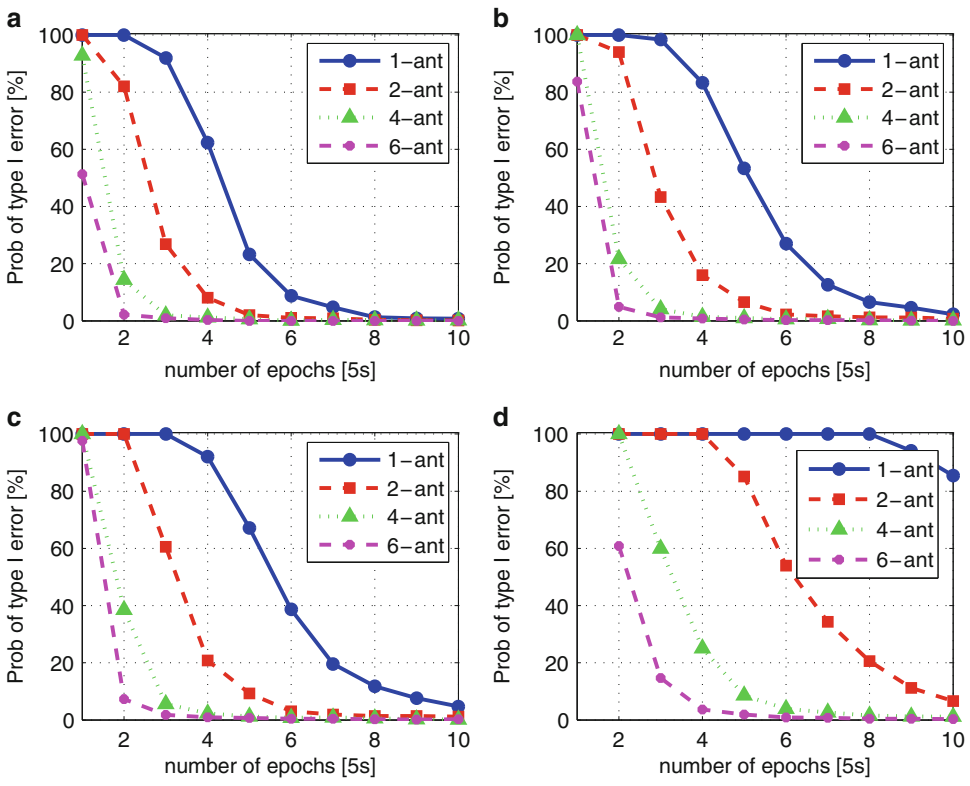

Fig. 5 The empirical probability P_{I} of the type I error for varying scenarios. The subplots (**a**–**d**) represent the results obtained with the DD ionospheric standard deviations, 10, 15, 20 cm and ∞

and

$$P_{\mathrm{II}} = \frac{\#\text{ accepted } (P_{\boldsymbol{B}} > 99.9\%) \text{ but wrong solutions}}{\#\text{ accepted solutions with } P_{\boldsymbol{B}} > 99.9\%} \tag{19}$$

Thus, with $P_{\boldsymbol{B}} < 99.9\,\%$ as the criterion for rejection, P_{I} describes the conditional rejection frequency of correct solutions, while P_{II} describes the conditional acceptance frequency of wrong solutions. Here, the correct/incorrect solutions are determined by comparing the solutions with the "true" integer ambiguities obtained from using all data of the complete time span. Note that the frequency of occurrence of correct solutions is related to P_{fix}, P_{I} and P_{II} as

$$P_{\mathrm{correct}} = P_{\mathrm{I}}(1 - P_{\mathrm{fix}}) + (1 - P_{\mathrm{II}})P_{\mathrm{fix}} \tag{20}$$

Figure 5 shows P_{I} for the varying experiment scenarios. As is clearly shown, the frequency of wrongful rejections is significantly reduced by using an array of antennas for all experiment scenarios. In particular, it is nearly 0 if 4 antennas are used with more than 3 data epochs for the three ionosphere-weighted models and with more than 6 epochs for the ionosphere-float model. However for the 1-antenna case, P_{I} is still larger than 20 % even if 5, 6 and 7 epochs are used with respect to the three DD ionospheric standard deviations of 10, 15 and 20 cm. Especially, for the 1 antenna ionosphere-float scenario it is nearly 100 % even if 8 epochs are used. Therefore, array-aided ambiguity resolution indeed improves the efficiency of ambiguity fixing. In a similar way it can be shown that array-aiding significantly reduces the occurrence frequency P_{II} of wrongful acceptance.

6 Concluding Remarks

A-PPP is a measurement concept that uses GNSS data, from multiple antennas in an array of known geometry, to improve GNSS model strength, thereby realizing a speed up in successful ambiguity resolution. In this contribution, the benefits of A-PPP has been explored for CORS network ambiguity resolution using antenna-array equipped CORS stations. The results from our 80 km baseline experiment show that between CORS-station ambiguity resolution can benefitsignificantly from the use of such antenna arrays. These improvements become more markedly, the weaker the underlying single-antenna model is. This is therefore in particular of interest for situations where the ionospheric constraints are weak or completely absent, such as may often be the case with CORS stations. Moreover, the probabilities of two types of errors (false alarm and missed detection) are reduced significantly by the antenna array, which means that the antenna array can improve the reliability of the ambiguity resolution. Therefore the array-aided CORS network ambiguity resolution has a high efficiency of ambiguity fixing and powerful to resist model errors.

Acknowledgements The second author is the recipient of an Australian Research Council (ARC) Federation Fellowship (project number FF0883188). Part of this work was done in the framework of the project "New Carrier-Phase Processing Strategies for Next Generation GNSS Positioning" of the Cooperative Research Centre for Spatial Information (CRC-SI2). All these supports are gratefully acknowledged. The members in GNSS Research Center are appreciated for their help to set up the GPS field experiment.

References

Buist P, Teunissen P, Giorgia G, Verhagen S (2011) Multivariate bootstrapped relative positioning of spacecraft using GPS L1/Galileo E1 signals. Adv Space Res 47:770–785

Giorgi G, Teunissen P, Verhagen S, Buist P (2010) Testing a new multivariate GNSS carrier phase attitude determination method for remote sensing platforms. Adv Space Res 46(2):118–129

Koch K (1999) Parameter estimation and hypothesis testing in linear models, 2nd edn. Springer, Berlin

Li B, Shen Y, Xu P (2008) Assessment of stochastic models for GPS measurements with different types of receivers. Chin Sci Bull 53:3219–3225

Teunissen P (1995) The least-squares ambiguity decorrelation adjustment: a method for fast GPS integer ambiguity estimation. J Geodes 70:65–82

Teunissen P (1998) Success probability of integer GPS ambiguity rounding and bootstrapping. J Geodes 72:606–612

Teunissen P (2006) Testing theory: an introduction. Series on mathematical geodesy and positioning, 2nd edn. Delft University Press, Delft

Teunissen P (2010) Integer least-squares theory for the GNSS compass. J Geodes 84:433–447

Teunissen P (2012) A-PPP: array-aided precise point positioning with global navigation satellite systems. IEEE Trans Signal Process 60(6):2870–2881

Verhagen S, Li B, Teunissen PJG (2013) Ps-LAMBDA: ambiguity success rate evaluation software for interferometric applications. Comp Geosci 54:361–376